AD-A148 672 DEFORMATION AND FRACTURE OF P/M (POWDER/METALLURGY) TITANIUM ALLOYS(U) MICHIGAN TECHNOLOGICAL UNIV HOUGHTON DEPT OF METALLURGICAL ENGINEERING D A KOSS 05 NOV 84 TR-27 N00014-76-C-0037 1/1

UNCLASSIFIED F/G 11/6 NL

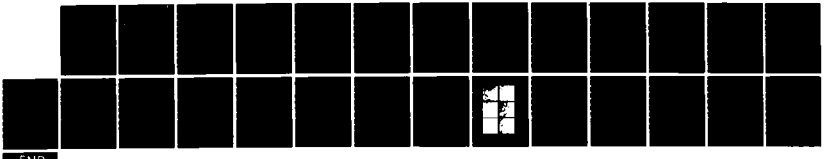

END

FILMED

DTIC

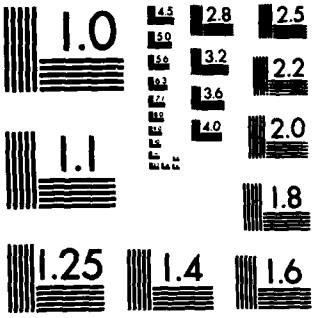

MICROCOPY RESOLUTION TEST CHART
NATIONAL BUREAU OF STANDARDS-1963-A

(12)

TECHNICAL REPORT No. 27
CONTRACT No. N00014-76-C-0037, NR 421-091

DEFORMATION AND FRACTURE OF P/M TITANIUM ALLOYS

DONALD A. KOSS
DEPARTMENT OF METALLURGICAL ENGINEERING
MICHIGAN TECHNOLOGICAL UNIVERSITY
HOUGHTON, MICHIGAN 49931

5 NOVEMBER 1984

ANNUAL REPORT FOR PERIOD 1 OCTOBER 1983 - 30 SEPTEMBER 1984

PREPARED FOR
OFFICE OF NAVAL RESEARCH
800 N. QUINCY STREET
ARLINGTON, VA 22217

SECURITY CLASSIFICATION OF THIS PAGE (When Data Entered)

REPORT DOCUMENTATION PAGE		READ INSTRUCTIONS BEFORE COMPLETING FORM
1. REPORT NUMBER 27	2. GOVT ACCESSION NO. AD-A148 672	3. RECIPIENT'S CATALOG NUMBER
4. TITLE (and Subtitle) Deformation and Fracture of P/M Titanium Alloys		5. TYPE OF REPORT & PERIOD COVERED Annual Report for 10/1/83 - 9/30/84 6. PERFORMING ORG. REPORT NUMBER
7. AUTHOR(s) Donald A. Koss		8. CONTRACT OR GRANT NUMBER(s) N00014-76-C-0037 NR 421-091
9. PERFORMING ORGANIZATION NAME AND ADDRESS Department of Metallurgical Engineering Michigan Technological University Houghton, Michigan 49931		10. PROGRAM ELEMENT, PROJECT, TASK AREA & WORK UNIT NUMBERS
11. CONTROLLING OFFICE NAME AND ADDRESS		12. REPORT DATE November 1984 13. NUMBER OF PAGES 23
14. MONITORING AGENCY NAME & ADDRESS(if different from Controlling Office)		15. SECURITY CLASS. (of this report) Unclassified 15a. DECLASSIFICATION/DOWNGRADING SCHEDULE

16. DISTRIBUTION STATEMENT (of this Report)

Distribution of this document is unlimited.

17. DISTRIBUTION STATEMENT (of the abstract entered in Block 20, if different from Report)

18. SUPPLEMENTARY NOTES

19. KEY WORDS (Continue on reverse side if necessary and identify by block number)

Ti alloys, powder metallurgy, ductile fracture, deformation, hydrogen embrittlement, porosity, hot isostatic pressing.

20. ABSTRACT (Continue on reverse side if necessary and identify by block number)

Progress is reviewed for a research program whose purpose is to provide a broad-based understanding of the application and consequences of certain advanced processing techniques to high performance alloys in general and to Ti alloys in particular. The research ranges from experimental studies of hot isostatic pressing (HIP) to experimental/analytical modeling of the deformation and fracture of materials with pre-existing porosity. Aspects of the search are also a fundamental study of fracture utilizing engineering

DD FORM 1 JAN 73 1473 EDITION OF 1 NOV 65 IS OBSOLETE
S/N 0102-LF-014-6601

SECURITY CLASSIFICATION OF THIS PAGE (When Data Entered)

materials containing processing-induced defects.

Progress for the period October 1, 1983 to September 30, 1984 is reviewed for the following portions of this research program:

1) the influence of porosity on the deformation and fracture of alloys over a wide range of strain rates;
2) the effects of void/pore distributions on ductile fracture as modeled by arrays of holes;
3) hot isostatic pressing of metallic powders; and
4) grain size/stress state effects on the hydrogen embrittlement of titanium.

INTRODUCTION

High performance alloys are used widely in applications requiring high strength and a good resistance to fracture in both inert and aggressive environments. Extending the use of these alloys is usually limited by certain characteristics of the alloy or by their high cost. The cost factor becomes especially important in components of complex shape where considerable material waste often occurs and extensive processing is required. This has led to the application of advanced processing techniques, such as powder metallurgy (PM), to high performance alloys. A problem inherent in these techniques is the possibility of processing-induced defects which, while not present in cast and wrought alloys, can seriously degrade the fracture resistance of the components. For example, powder-fabricated or cast Ti alloys may contain defects, such as porosity, not normally present in their cast and wrought counterparts.[1-4]

The primary purpose of the proposed research is to provide a broad-based understanding of the application and consequences of certain advanced processing techniques to high performance alloys in general and to Ti alloys in particular. The research ranges in scope from experimental studies of hot isostatic pressing (HIP) to experimental/analytical modeling of the deformation and fracture of materials with pre-existing porosity. It should be noted that much of research is also a fundamental study of fracture utilizing engineering materials containing processing-induced defects. Substantial progress has been achieved in this research program during the period October 1, 1983 to September 30, 1984 in the following areas:

1) the influence of porosity on the deformation and fracture of alloys over a wide range of strain rates,

2) the effect of void/pore distributions on ductile fracture as modeled by arrays of holes,

3) hot isostatic pressing of metallic powders,

and 4) grain size/stress state effects on the hydrogen embrittlement of titanium.

An important aspect of this program is the educational experience it provides the graduate students involved. The following students have been supported by this program during part or all of the past fiscal year: Barbara Lograsso, Ph.D. candidate, Stephen Kampe, Ph.D. candidate, Paul Magnusen, Ph.D. candidate, Dale Gerard, M.S. candidate, and Ellen Dubensky, M.S. candidate.

The Influence of Porosity on the Deformation and Fracture of Alloys Over a Wide Range of Strain Rates (with Roy Bourcier and Paul Magnusen, also Dr.'s O. Richmond and R. Smelser, Alcoa Laboratories, and P. Follansbee, Los Alamos National Laboratory)

Ductile fracture in engineering alloys is usually the result of the nucleation, growth and link-up of voids or cavities. In fully dense materials, voids are formed during straining, usually by the decohesion or fracture of large inclusions or precipitates (for a review, see Goods and Brown[5]). While the statistical nature of void formation results in cavities being nucleated over a range of strains, void nucleation in most alloys begins early in the deformation process, and as a result the fracture behavior is controlled by void growth and void link-up. Furthermore, many technologically important materials contain pre-existing porosity, such as may be present in castings and powder metallurgy (P/M) consolidated alloys. The present research is an examination of the effects of pre-existing porosity and of matrix strain hardening on the deformation and fracture of high strength engineering alloys in general and of two P/M Ti alloys in particular.[6,7]

The influence of porosity on plastic flow and instability/fracture has been studied experimentally (for a review, see refs. 8 and 9), with physical models,[10-12] with simple models based on elastic stress concentrations and an assumed pore geometry in sintered metals,[13-19] and with mathematical models (for example, see refs. 20-25). A limitation of previous studies is that little critical comparison has been made between models which take into account plasticity and the observed flow and fracture behavior of the porous material. The result is that the validity of the modeling techniques (especially at large strains) remains unproven, and no basis exists to suggest modifications or improvements. The purpose of this study is not only to identify the parameters which control the deformation and fracture of porous or cavitating alloys but also to relate these to experimental data. In particular, the research distinguishes between behavior which may be adequately interpreted in terms of bulk porosity content and that which is dominated by planes of high local pore content.

The experimental aspects of the study are based on the contrasting deformation and fracture behavior of two Ti alloys, commercially pure (CP) Ti and Ti-6Al-4V, which possess considerably different strain-hardening characteristics and which have been consolidated via P/M techniques to similar levels of rounded and mostly isolated porosity. The yielding, flow, and void growth behavior have been examined experimentally over a range of strain rates from 10^{-4} to $10^{2}s^{-1}$. The results are subsequently analyzed on two levels: (1) a bulk porosity basis simulated by a large strain elastic-plastic finite element model and (2) a local porosity basis in which the material is viewed in terms of planes of high pore content: "imperfections".

Both the tensile deformation and fracture of powder-fabricated Ti-6Al-4V, commercially pure Ti, and Ni were investigated at porosity levels from

near-fully dense to ~9%. The principal results may be summarized as follows:[6,7]

(1) Increasing porosity causes decreases in the (a) yield stresses (which exceed those predicted by the rule of mixtures), (b) ductility, and (c) strain hardening exponent. In all three cases, the decreases are most pronounced in the materials [Ti-6Al-4V] with the smallest work hardening rate.

(2) At all porosity levels, the fracture surface is characterized by a much higher pore content (roughly from 4x to 10x, depending on material) than is present on a random plane in the bulk. The large amount of porosity on the fracture surface cannot be accounted for by strain-inducted pore growth.

(3) Over a range 10^{-4} to $10^{2}s^{-1}$, the strain rate has only minor effects on either the uniform strain, local fracture strain, or tensile elongation to failure. The absence of any strong effect on fracture at any level of porosity may be understood in terms of the lack of any strong rate sensitivity of void formation, growth, and link-up at room temperature and in terms of the rate-insensitivity of the failure process involving shear instabilities developing along planes of high pore content.

(4) Two minor ductility effects are observed in the strain-range range examined. The first, a weak minimum in elongation to failure in Ti containing 0.1 and 1.5% porosity, appears to be caused by thermal gradients developing due to diffuse necking and incomplete heat dissipation along the specimen length. The second, a small ductility increase at high strain rates in Ni, appears to be caused by a

combination of increased strain-rate sensitivity and decreased susceptibility to hydrogen embrittlement at high strain rates.

The decrease in tensile ductility with increasing porosity is both pronounced and technologically important. There appear to be two mechanisms which contribute to the loss of ductility: (1) a decrease in uniform elongation due to the combination of pore growth (a "bulk" porosity effect) and a porosity-induced decrease in work hardening rate [see Fig. 1[6]] and (2) porosity-triggered shear instabilities which occur at large strains and are caused by planes of high local pore content ("imperfections").[7] In the latter case, the analysis of Saje, Pan, and Needleman[26] may be used to predict the total fracture strain of the material;[7] Fig. 2 shows that again good agreement is obtained between theory and experiment.

The Effect of Void/Pore Distributions on Ductile Fracture as Modeled by Arrays of Holes (with Ellen Dubensky)

The above study shows the pre-existing porosity or strain-induced voids can introduce planes of weakness into the materials. These "imperfections" can subsequently trigger a shear instability which creates microvoid sheets and final failure. Obviously, the distribution of pores/voids (or other processing "defects" such as non-uniform microstructures) is an important an often the controlling parameter in determing the resistance to tensile fracture. The purpose of this study is to model experimentally the influence of void/pore distributions on ductile fracture. The only previous research concerning fracture in a material with a random distribution of voids is a theoretical analysis developed by Melander[27] who used computer simulation to apply his theory to two arrays of voids; no experimental verification was attempted. Thus the present research is also the first aimed at developing a

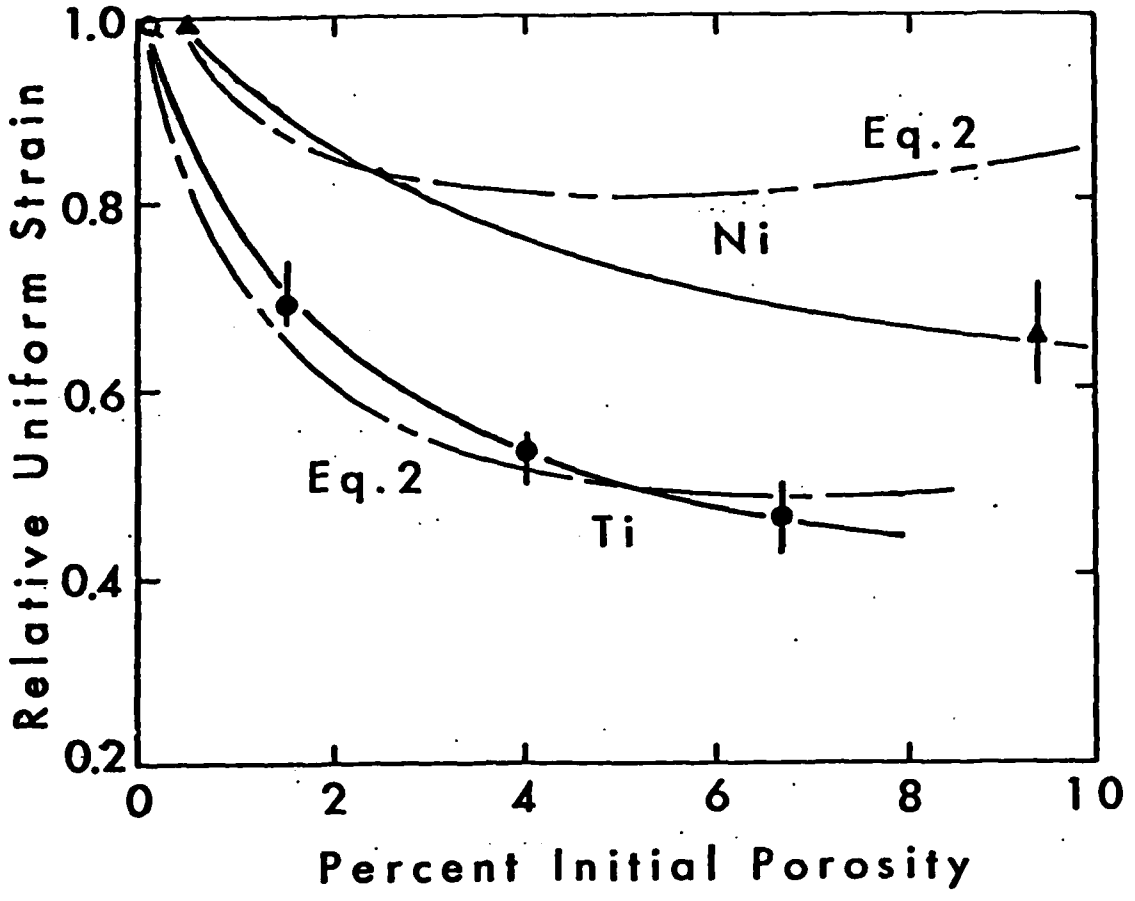

Fig. 1. The influence of porosity f_o on the relative uniform strain, which is defined as the strain ε_u at the onset of diffuse necking (maximum load) for a porous material divided by that of a fully dense compact. Eq. 2 is $\varepsilon_u \simeq n(1-f_o)/(1-f_o-af_o)$ where n is the strain hardening exponent and a is a constant determined by the rate of strain-induced pore growth[6].

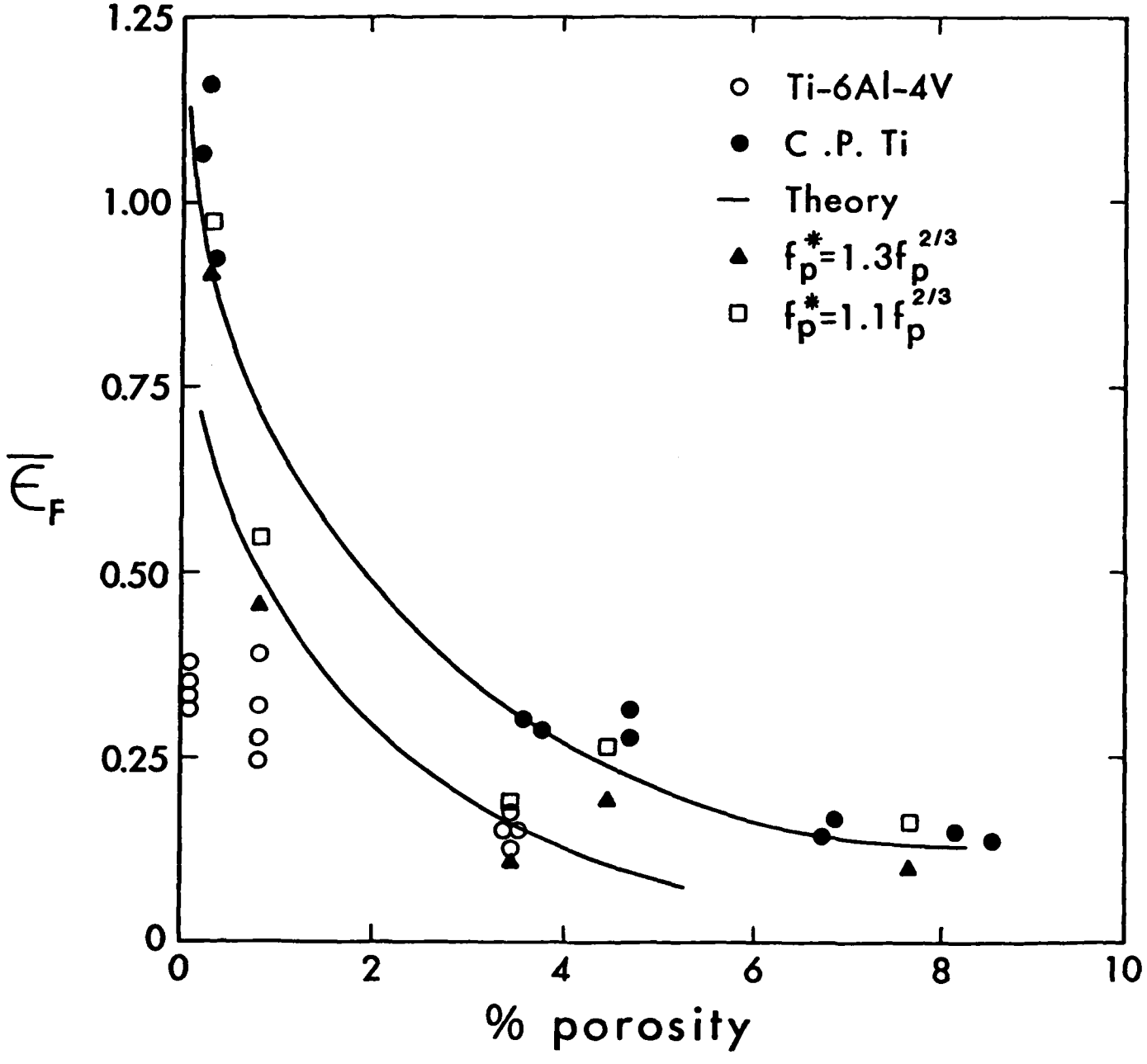

Fig. 2. The dependence of strain to fracture $\bar{\epsilon}_f$ on porosity content. The experimental data is compared to the prediction of the continuum imperfection analysis[26] based on imperfections resulting from planes of high pore content whose area fraction of porosity f_p^* is related to that in the bulk f_p by either $f_p^* = 1.1\ f_p^{2/3}$ or $f_p^* = 1.3\ f_p^{2/3}$; see ref. 7.

sound experimental basis for the theory of ductile fracture as influenced by void distribution.

In the present study, void distributions are modeled in two dimensions as arrays of holes whose positions are predicted by a random-number generator in an appropriate computer program; for an example, see Fig. 3. Initially, the experiments are being conducted on arrays of equi-sized holes in which the (a) area fraction of holes F, (b) diameter of the holes D, and (c) minimum spacing of the holes S_m is controlled. The study is based on two materials (1100 Al and 7075 Al) of differing work hardening rates which are tested under conditions of plane stress vs. plane strain: (a) 1100-0 Al in the form of 1 mm sheet (plane stress deformation), (b) 7075-T6 Al also as 1 mm sheet and (c) 7075-T6 Al plate (~6 mm thick) in which deformation between the holes is predominantly plane strain. The test matrix shown in Table I indicates the values of F, D, and S_m used in this study. Three different random arrays are generated and tested for each combination of D, L_m, and f_H. A total of 72 specimens thus are being tested in uniaxial tension; one specimen in each condition is gridded for local strain determinations and all specimens are photographed during testing.

Table I. Experimental Values of Hole Diameter D, Area Fraction of Holes F, and Minimum Inter-hole Spacing S_m Examined

S_m \ D	1.2 mm (-)	2.0 mm (+)
0.5 mm (-)	F = 2.5% (-) 5.0% (+)	F = 2.5% 5.0%
2.0 mm (+)	2.5% 5.0%	2.5% 5.0%

RANSET1A

145 HOLES. D=1.2MM. S=0.5MM. F=5%

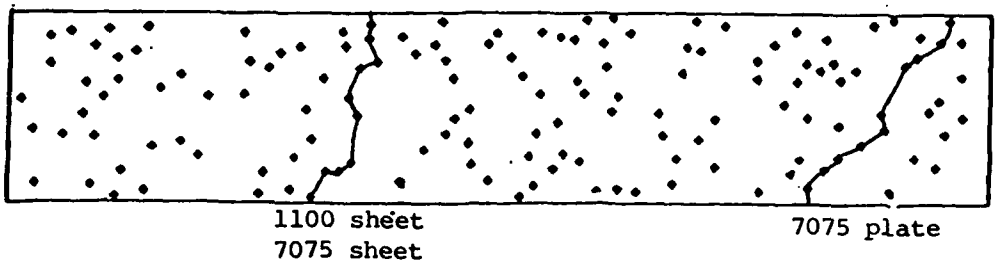

RANSET1B

145 HOLES. D=1.2MM. S=0.5MM. F=5%

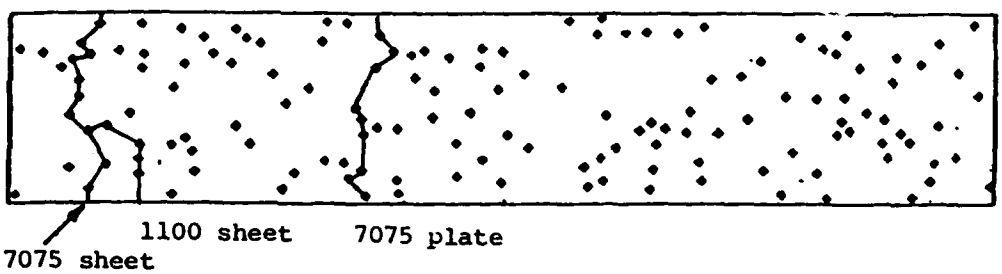

RANSET1C

145 HOLES. D=1.2MM. S=0.5MM. F=5%

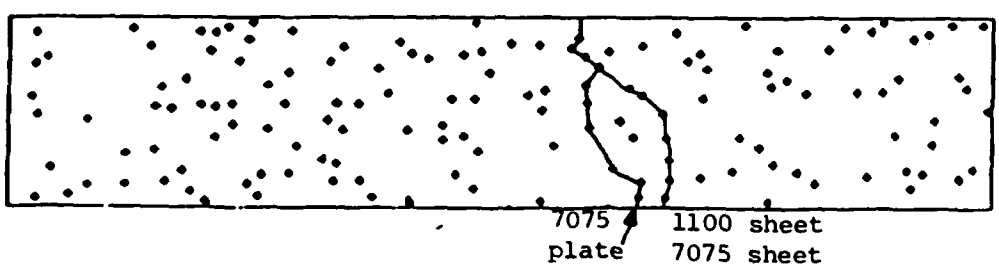

Fig. 3. A schematic showing positions of 145 holes, each having a diameter 1.2 mm and a minimum spacing 0.5 mm, drilled through the thickness of tensile specimen. Fracture paths across the test specimens are indicated.

The experiment technique is based on a 2^3 factorial design in which 2 levels (values) are chosen for each of 3 factors (parameters) D, F and S_m, and tests are performed for all possible combinations. Table 1 shows the "+" and "-" levels for each parameter. As a measure of experimental error, three different random arrays have been generated for each D, F and S_m combination; Fig. 3 shows examples of three different arrays for a specific set of D, F, and S_m conditions.

The factorial analysis permits an estimation of the "effects" of the hole distribution parameters D, S_m, and F as well as their interactive effects (DS_m, DF, S_mF, and DS_mF) on the resulting mechanical properties <u>within</u> the range of D, S_m, and F values in Table I. In the present case, the engineering strain to failure e_f and the yield stress σ_y are of primary interest, although the engineering stress at maximum load σ_m has also been examined. The analysis thus provides the mean magnitudes of the coefficients a, b,...h in the following linear relationship:

$$e_f,\ \sigma_y,\ \text{or}\ \sigma_m = \frac{a}{2} + \frac{b}{2}D + \frac{c}{2}S_m + \frac{d}{2}F + \frac{e}{2}DS_m + \frac{f}{2}DF + \frac{g}{2}S_mF + \frac{h}{2}DS_mF. \qquad (1)$$

Using the 2^3 factorial design, the magnitude of a particular coefficient can be obtained by comparing the magnitude of a property (e_f, σ_y, or σ_m) at the (+) or (-) levels of D, S_m and F as indicated in Table I. For example, the estimated effect of hole diameter D on fracture strain e_f is: ($\bar{e}_f$ at D = 2.0 mm (+)) - ($\bar{e}_f$ at D = 1.2 mm (-)), where e_f is the mean fracture strain for the three tests at each condition.

A hole distribution parameter is determined to have a <u>significant</u> effect on a property if the estimated effect of that parameter is sufficiently larger

than the standard experimental error.* This is illustrated in Table II for the case of fracture strain in the 1100-0 Al sheet. For example, as shown in Table II,

Table II. The dependence of fracture strain e_f(%) for the range of hole distribution parameters listed below

Parameter(s)+	Coefficient	Effect ± Std. Error
Mean	a	7.85 ± 0.19%
D	b	-1.46 ± 0.38
S_m	c	0.92 ± 0.38
F	d	-0.05 ± 0.38
DS_m	e	-0.31 ± 0.38
DF	f	0.03 ± 0.38
$S_m F$	g	-0.36 ± 0.38
$DS_m F$	h	0.34 ± 0.38

+For the range: D = 1.2 or 2.0 mm; S_m = 0.5 or 2.0 mm, F = 2.5 or 5.0%

increasing the hole diameter D in the 1100-0 sheet from 1.2 to 2.0 mm at constant S_m and F causes a decrease of e_f by 1.46 ± 0.38%. Inspection of Table II shows that this and the influence of minimum hole spacing S_m are the only parameters which result in significant effects on ductility of the 1100-0 Al sheet whereas the area fraction of hole F and interactive effects are insignificant (compare the magnitudes of the effects with the standard errors in Table II). It must be emphasized that these conclusions are based on the data analysis for the range of conditions in Table I. Thus while the area fraction of holes undoubtedly affects fracture strain, its influence from F = 2.5 to 5.0% is small.

*For a given property, the standard error for coefficients b through h in Eq. 1 is based on a pooled estimate of the variance among three different random arrays with identical values of D, S_m, and F. To estimate the pooled variance σ^2, the individual variances for each D, S_m, and F condition are summed and divided by the number of degrees of freedom.

To date the 1100-0 Al sheet [plane stress, high strain hardening] and 7075-T6 Al plate [plane strain between holes, low strain hardening] have been tested and analyzed; preliminary data on 7075-T6 sheet is also available. Using the analysis procedures described above, the coefficients in Eq. 1 for e_f, σ_y, and σ_m have been determined for these two materials and stress-state conditions and compared to the standard error for that property. Those parameters which are statistically significant over the range of D, S_m, and F-values tested are summarized in Table III.

Table III. The magnitudes of the coefficients (see Eq. 1) of those hole distribution parameters which are significant in influencing fracture strain e_f, yield stress σ_y, and stress at maximum load σ_m. The ranges of hole parameters are: D = 1.2-2.0mm, S_m = 0.5-2.0mm, and F = 2.5-5.0%.

Property	Material	D	S_m	F	Interactions
e_f(%)	1100 Sheet	-1.5 ± 0.4	0.9 ± 0.4		
	7075 Sheet	-0.3 ± 0.1			
	7075 Plate	0.4 ± 0.2	0.8 ± 0.2		(0.5 ± 0.2)DS_m
σ_y(MPa)	1100 Sheet	-5.0 ± 1.4	4.6 ± 1.4	-3.0 ± 1.4	
	7075 Sheet			-30.0 ± 5.6	
	7075 Plate	-20.8 ± 4.9	17.2 ± 4.9	-33.1 ± 4.9	
σ_m(MPa)	1100 Sheet		4.8 ± 1.7		
	7075 Sheet	-22.3 ± 5.0	19.6 ± 5.0	-27.9 ± 5.0	
	7075 Plate	-28.3 ± 7.5	34.6 ± 7.5	-23.6 ± 7.5	

The results in Table III indicate several conclusions:

(1) With the exception of the 7075 sheet which shows very little ductility in any condition, increasing the minimum hole spacing S_m increases both the strength and the ductility of the materials examined thus far.

(2) An increase in hole size (from 1.2 to 2.0mm) causes a modest decrease in ductility and a comparatively larger decrease in the yield and failure strengths.

(3) Increasing the area fraction of holes from 2.5 to 5.0% causes a rapid decrease in the strength of the 7075-T6 plate and sheet. The ductilities of all three materials are statistically unaffected in range 2.5-5.0%.

(4) Only one interaction term is noted: $e_f = f(DS_m)$ for the 1100-0 Al. Specifically, the loss of ductility with decrease S_m is greater for the 1.2 mm holes than for the 2.0 mm holes.

(5) As is illustrated in Fig. 3, the fracture path depends primarily on the stress state between holes and is nearly independent of matrix strain hardening. "Plane-stress" fractures in the 1100 and 7075 sheet follow near-identical paths roughly normal to the maximum principal stress axis. In contrast, the "plane-strain" fracture paths tend to be more tortuous with many ligaments oriented ~45° to σ_1.

Some (tentative) inferences may be drawn as regards ductile fracture of metals (or failure of panels or plates containing multiple holes). First, minimum hole (void) spacing, or the degree of clustering, exerts a very strong influence on the flow and fracture of materials which contain either pre-existing porosity or may easily form voids at inclusion. The effect is such that increasing minimum hole spacing [rendering hole spacings more uniform] usually increases both strength and ductility, especially when plane strain deformation between holes exists, as in the case of 7075-T6 plate. This is demonstrated in Fig. 4 in which the yield strength and ductility of panels containing equally-spaced, regular arrays of holes are compared to data from random arrays; note the influence of "nearest neighbor spacings". Secondly, hole size appears to have a strong influence on yield and tensile strength; this suggests an importance of the scale of the plastic zones adjacent to holes/voids with regard to the dimensions of the ligament between holes/voids. This is demonstrated by the catostrophic fracture of the 7075-T6 Al plate

REGULAR ARRAYS

D=1.2mm, F=5%

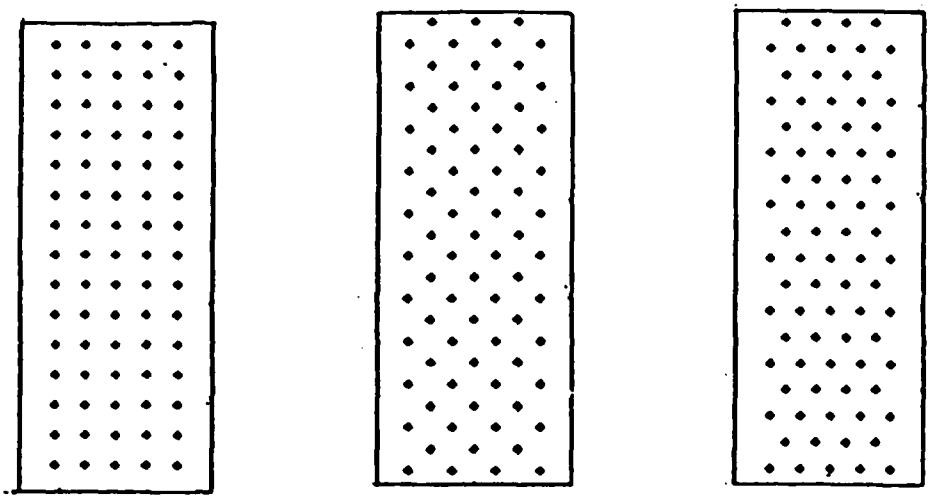

SQUARE DIAGONAL HEXAGONAL

COMPARISON BETWEEN REGULAR AND RANDOM ARRAYS

ARRAY	e_f (%)	σ_y (MPA)	Nearest Neighbor Spacing (mm)
Square	7.5	497	2.9
Diagonal	5.3	474	2.9
Hexagonal	5.9	502	2.9
Random S=2.0mm	2.8	460	2.0
Random S=0.5mm	1.2	431	0.5

Fig. 4. A schematic showing hole configurations of three regular arrays of holes as well as resulting ductility and yield strength data for 7075-T6 Al plate. Data for random arrays is included for comparision; note the decrease in ductility when the holes are random.

specimens after one or two ligaments fail, probably due to a shear instability between closely-spaced, oriented holes.

Confirmation of the above analysis depends on a more complete analysis of the results and on extending the range of hole contents. This would obviously provide a much better indication of the validity of our inferences, especially with regard to the influence of the area fraction of holes/voids.

Hot Isostatic Pressing (with Barbara Lograsso)

The use of hot isostatic pressing (HIP) to compact both powders and castings to full density has been a commercial practice for more than a decade. Over that time period, the pressure-time-temperature conditions required to achieve a fully dense material have been developed by each industrial user on an empirical basis. Most of the published data currently available concerns the pressure-time-temperature conditions required to achieve a 100% dense compact. Only the very recent study of Swinkels, Wilkinson, Arzt, and Ashby examines HIP over a range of densities and those data are only for lead, tin, and PMMA.[28] In this study, little attention was devoted in that study to the role of interparticle bonding, and the experimental conditions chosen were such that diffusional sintering, which results in rounding of porosity and densification, was ignored. This study seeks to establish pressure-time-temperature relationships which characterize HIP for a range of metallic powders which exhibit different degrees of interparticle bonding. The results test and extend existing theories, and provide a basis for more efficient utilization of HIP and for understanding HIP-induced effects. This could be particularly important in the consolidation of rapidly solidified powders in which low temperatures - short times may be crucial to retaining the superior properties inherent in such powders.

In this present study, four powder materials (commercially pure titanium, Ti-6Al-4V, nickel, and 316 stainless steel) are being HIP'ed over a range of temperatures, pressures and times to determine the pressure-temperature-time final density relationships. To facilitate the HIP'ing, the powder is being hermetically sealed in metal cans, copper for T>900 C and a steel for T<900 C. To protect the powder from reacting with the can, the powder is wrapped in a tantalum pouch. The filled cans are then outgassed, crimped and the ends are welded. The compaction is performed in a ASEA Mini-Hipper pressure vessel using argon gas as the compressing medium for pressures up to 205 MPa and temperatures up to 1500°C. The influence of powder shape and size and the degree of interparticle bonding is also being examined. For the experiments, a factorial design approach is being employed so that relatively few tests are performed per variable (time, temperature, pressure, powder size). Furthermore, this encourages the use of a sequential approach consisting of setting the initial design, testing, and then reassessing the design as the results of each group of data becomes available.

Preliminary results for the four metallic powders being examined are shown in Table IV below, but more data is obviously required before pressure-time-temperature-final density relationships may be established. The inter-particle bonding and densification process can also be qualitatively examined on the basis of the associated fracture surfaces. Figure 4 shows a comparison of Ni to Ti-6Al-4V under similar pressure-time-temperature conditions. The behavior of these two materials can be explained in terms of the operating mechanisms for densification during HIP'ing: diffusional creep at low stresses, power-law creep at higher stresses, plastic flow at yet higher stresses as well as diffusional sintering at high temperatures. For example, we may compare the HIP behavior of Ti-6Al-4V to that of Ni at 700°C, by noting

that the much higher flow stress of the titanium alloy at 700°C (~220 MPa verses ~60 MPa for Ni) results in a lower densification rate for Ti-6Al-4V. At 800°C, the flow stress of Ti-6Al-4V decreases to ~80 - 120 MPa which is comparable to 316 stainless steel but still greater than ~40 MPa for Ni. Despite a similar flow stress at 800°C, Table IV shows that the Ti alloy has more rapid densification than the stainless steel. This behavior can be attributed to two effects: (a) Ti alloy has a higher diffusivity than either Ni or 316 stainless steel at 800°C, (b) the Ti alloy is able to dissolve its oxide. The higher diffusivity results in more rapid densification by creep as well as diffusional sintering as powder particles undergo interparticle bonding [compare Ni to Ti-6Al-4V in Fig. 5].

Table IV. Final Densities of Four Metallic Powders Subjected to the Indicated HIP Conditions.

Temperature	900°C	800°C				700°C
Pressure	103MPa	103MPa		35MPa		35MPa
time / Powder	1 hr	1 hr	9 hrs	1 hr	9 hrs	1 hr
316 S. Steel T_{mp}=1375-1400°C	96.8%	82.3%	90.0%	69.2%	70.6%	
CP Ti T_{mp}=1660°C	100	97.8	100	96.4	-	76.7
Ti-6Al-4V (T_{mp}=1600°C-1660°C)	99.1	97.8	99.5	90.2	92.6	72.4
Ni(T_{mp}=1435°C)	98.2	97.2	98.4	85.0	86.8	75.0

Note: All material Plasma Rotating Electrode Powder (spherical); the 316 S/S, Ti-6Al-4V, and CP Ti powder particles are in the size range: -70 to +100 mesh, and the Ni is -100 to +140 mesh.

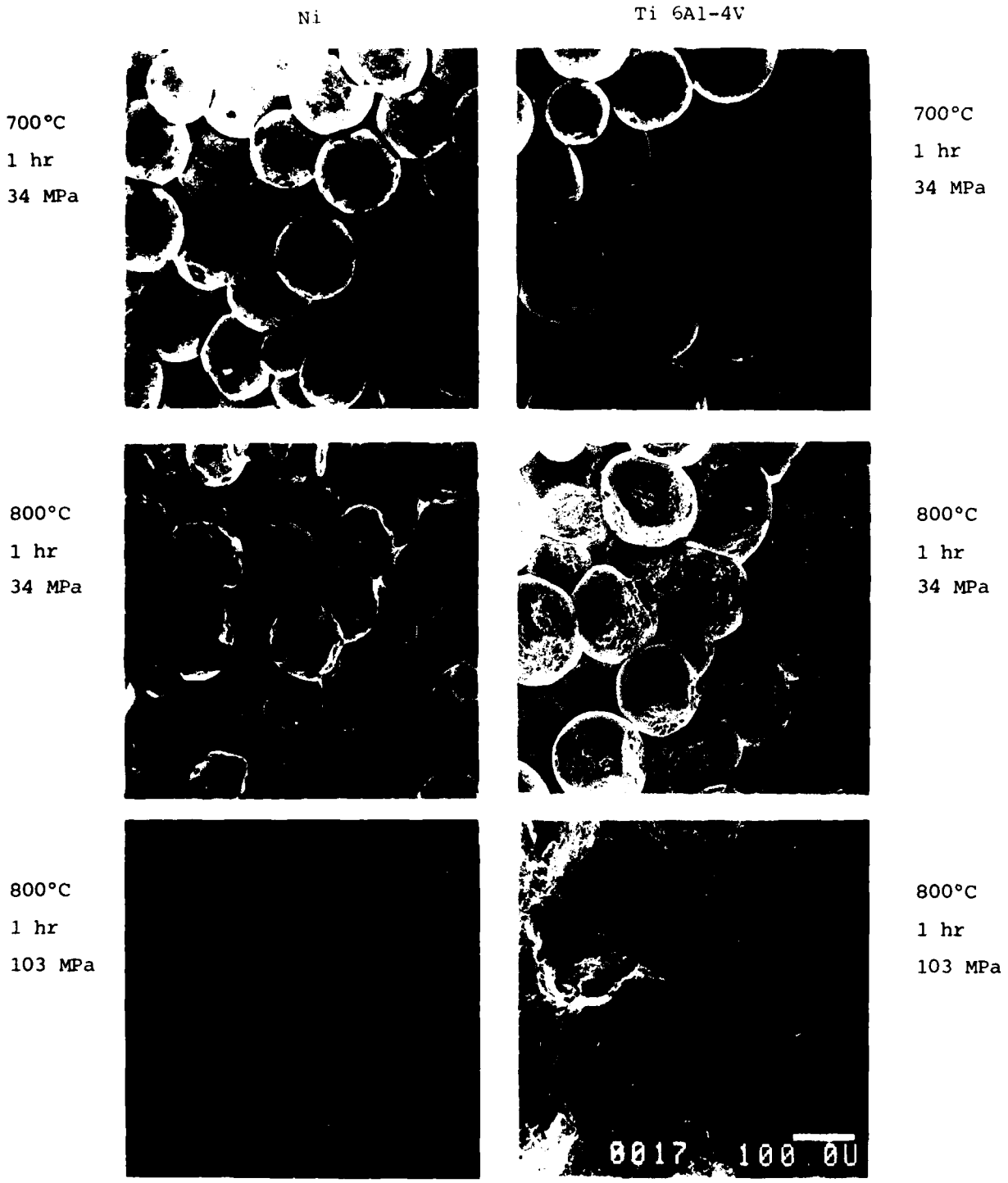

Fig. 5 Scanning electron micrographs of Ni and Ti-6Al-4V powder particles after HIPing under the conditions noted. All micrographs are the same magnification; note 100 μm marker.

Research is currently underway to determine the degree of interparticle bonding on a comparative basis as in Fig. 5, to extend the range of pressures and times for the HIP cycles in Table IV, and to separate the densification due to sintering from that of diffusional creep.

The Effect of Plastic Anisotropy and Grain Size on the Hydrogen Embrittlement of Titanium Sheet (with Dale Gerard)

In a previous study, by Bourcier and Koss,[29] the influence of hydrogen on the ductility of commercially pure (CP) titanium sheet has been investigated over a range of stress states from uniaxial to equibiaxial tension. Those data show that hydrogen embrittlement (HE) of plastically anisotropic Ti sheet depends on stress state, being most severe in equibiaxial tension. Quantitative metallography indicated that the effect of stress state was related to the acceleration of (1) void formation due to strain-induced hydride fracture under equibiaxial tensile deformation and (2) void link-up in equibiaxial tension occuring at a small void density. The comparative ease of void formation in equibiaxial tension was in turn believed to be a consequence of the large degree of plastic anisotropy in the Ti sheet examined in the previous study. Thus the objective of this study is to examine the effect of hydrogen embrittlement of titanium sheet having low degree of plastic anisotropy. In such sheet material, the maximum principal stress obtained under multiaxial loading conditions should be nearly equal to that in uniaxial tension. It was hoped that this would identify a means of reducing the sensitivity of this hydrogen embrittlement process to stress state.

A thermomechanical treatment has been developed to break down the texture of the titanium sheet. As a result, the plastic anisotropy ratios have been reduced from R=2.3, P=5.8 to R=1.3, P=1.3 [R=P=(width strain)/(through-thickness strain), where R and P are measured from uniaxial tension specimens

with the tensile axes parallel to the rolling, and transverse directions respectively]. When R and P are equal to 1.0 the material should be isotropic; therefore the thermomechanically treated sheet may be termed "near-isotropic".

Figure 6 shows the degree of the hydrogen embrittlement of the near-isotropic and anisotropic titanium sheet containing 1200 ppm hydrogen. The results are unexpected, revealing that the near-isotropic material is more susceptible to HE in both uniaxial and equibiaxial tension. This increase in sensitivity to HE appears to be due to a larger grain size present in the near-isotropic sheet (30 vs. 15 μm). Initially, the difference in grain size was believed to be insignificant. However, the larger grain size allows larger hydrides to form, and the concomitant reduction in the grain boundary area results in a larger fraction of the grain boundary area being covered with hydrides since a large fraction of the hydrides are intergranular. The larger hydrides appear to fracture at smaller strains enhancing void initiation, and the extensive network of (large) grain boundary hydrides enhances void link-up in the sheet in the coarse grain material. Therefore, it appears that premature void initiation and enhanced void link-up can make hydrogen embrittlement more severe with increasing grain size at least at high hydrogen contents. While grain size effects have been noted previously, the effect in uniaxial tension was believed to be small.[30] However, given the sensitivity of fracture in equibiaxial tension to void link-up, the grain size effect may be quite pronounced in multiaxial tensile states of stress.

In order to confirm the significance of grain size as well as to assess properly the influence of plastic anisotropy on hydrogen embrittlement, we are currently examining the embrittlement of titanium sheet of varying grain size but near-constant plastic anisotropy. Tests are being performed in uniaxial and equibiaxial tension to determine whether the grain size effects are indeed most pronounced in equibiaxial tension as suspected.

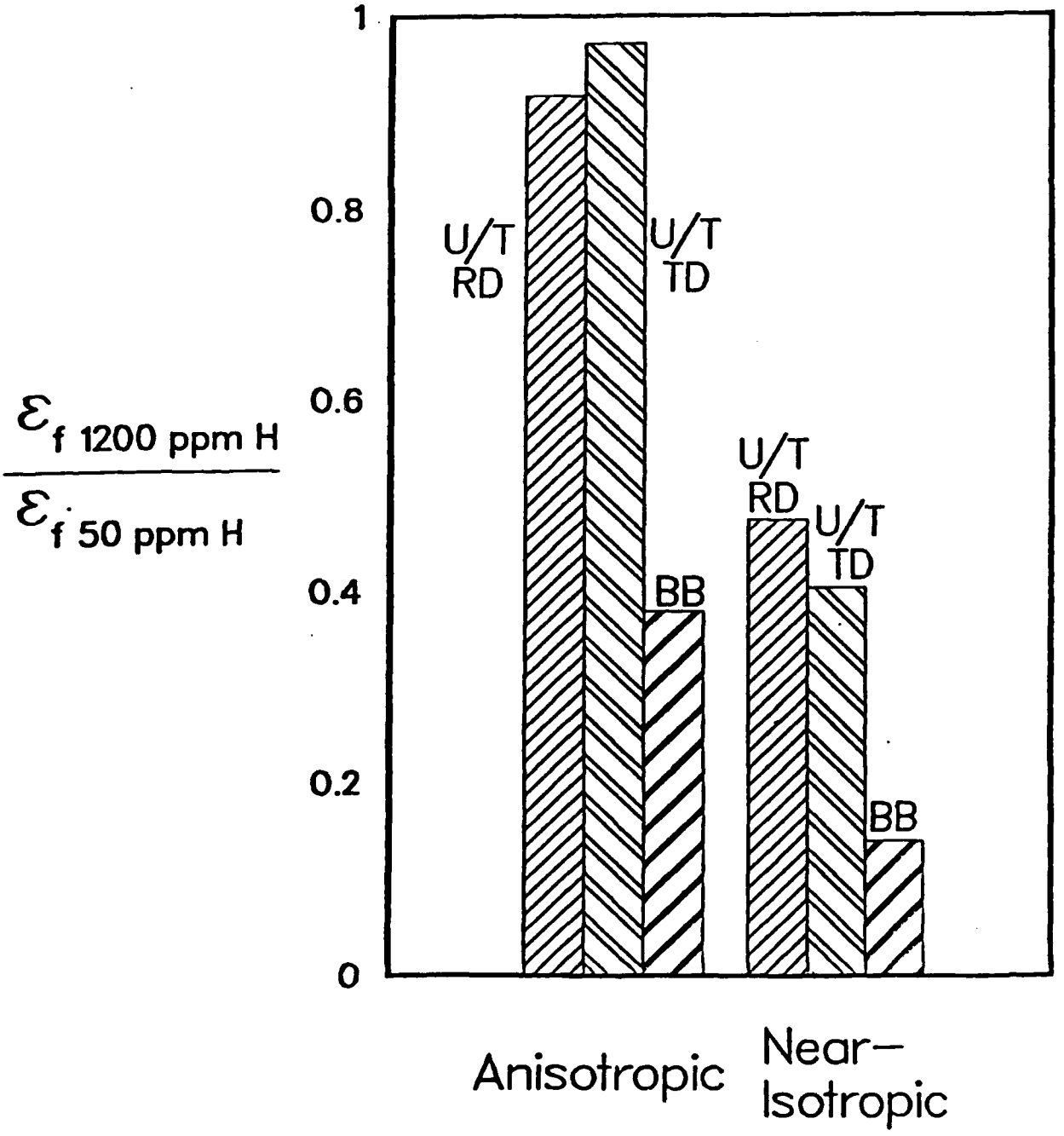

Fig. 6. The ratio of the local strain to fracture at 1200 ppm H versus that at 50 ppm H for Ti tested in uniaxial tension (U/T) in both the rolling (RD) and transverse (TD) directions and in balanced biaxial tension (BB).

REFERENCES

1. Titanium Powder Metallurgy, F. H. Froes and J. Smugeresky, eds., TMS-AIME, Warrendale, PA, 1980, p. 1-314.

2. F. H. Froes, D. Eylon, G. E. Eichelman, and H. M. Burte, J. of Metals 32, 49(1980).

3. S. Krishnamurthy, R. G. Voght, D. Eylon, and F. H. Froes, in Proc. 1983 MPIF/APMI Annual Conf., May, 1983.

4. D. Eylon in Titanium Net-Shape Technologies, to be published by TMS-AIME, 1984.

5. S. H. Goods and L. M. Brown, Acta Metall. 27, 1 (1979).

6. P. E. Magnusen, P. S. Follansbee, and D. A. Koss, "The Influence of Strain Rate and Porosity on the Deformation and Fracture of Titanium and Nickel", Technical Report No. 25, ONR Contract N00014-76-C-0037, NR 031-756, July, 1984

7. R. J. Bourcier, D. A. Koss, R. E. Smelser, and O. Richmond, "The Influence of Porosity on the Deformation and Fracture of Alloys", Technical Report No. 26, ONR Contract N00014-76-C-0037, NR 031-756, Nov., 1984.

8. R. Haynes, The Mechanical Behavior of Sintered Alloys, Freund Publishing House, London, 1981.

9. B. Karlsson and I. Bertilsson, Scand. J. of Met. 11, 267 (1982).

10. M. Perra and I. Finnie, in Fracture 1977, Vol. 2, p. 415, Univ. of Waterloo Press, Waterloo, 1977.

11. R. J. Bourcier and D. A. Koss, in Advances in Fracture Research, Vol. 1, p. 187, Pergamon Press, London, 1982.

12. R. J. Bourcier, R. E. Smelser, O. Richmond and D. A. Koss, Intern. J. of Fracture 24, 289 (1984).

13. M. Eudier, Powder Metall. 6, 278 (1962).

14. B. I. Edelson and W. M. Baldwin, Trans. ASM 55, 230 (1962).

15. A. Salak, V. Miskovič, E. Dubrová, E. Rudnayoua, Powder Metall. Intern. 6, 128 (1974).

16. R. Haynes, Powder Metall. 20, 17 (1977).

17. H. E. Exner and D. Pohl, Powder Metall. Intern. 10, 193 (1978).

18. T. J. Griffiths, R. Davies, and M. B. Bassett, Powder Metall. 22, 119 (1979).

19. N. A. Fleck and R. A. Smith, Powder Metall. 24, 126 (1981).

20. F. A. McClintock, J. Appl. Mech. 35, 363 (1968).

21. J. R. Rice and D. M. Tracey, J. Mech. Phys. Solids 17, 201 (1969).

22. A. Needleman, J. Appl. Mech. 35, 964 (1972).

23. A. Melander, Acta Met. 28, 1799 (1980).

24. P. F. Thomason, Acta Metall. 29 763 (1981).

25. V. Tvergaard, Intern. J. Frac. 17, 389 (1981) and 18, 237 (1982).

26. M. Saje, J. Pan, and A. Needleman, Intern. J. of Fracture 19, 163 (1982).

27. A. Melander, Mat'l. Sci. and Eng. 39, 57 (1979).

28. F. B. Swinkels, D. S. Wilkinson, E. Arzt, and M. F. Ashby, Acta Metall. 31, 1829 (1983).

29. R. J. Bourcier and D. A. Koss, Acta Metall. (in press).

30. C. J. Beevers and D. V. Edmonds, Trans. AIME 245, 2391 (1969).

END

FILMED

1-85

DTIC